Acta Pharmacologica Sinica (2016) 37: 1359–1369
 1671-4083/16
www.nature.com/aps

Original Article

OL3, a novel low-absorbed TGR5 agonist with reduced side effects, lowered blood glucose via dual actions on TGR5 activation and DPP-4 inhibition

Shan-yao MA, Meng-meng NING, Qing-an ZOU, Ying FENG, Yang-liang YE, Jian-hua SHEN*, Ying LENG*

State Key Laboratory of Drug Research, Shanghai Institute of Materia Medica, Chinese Academy of Sciences, Shanghai 201203, China

Aim: TGR5 agonists stimulate intestinal glucagon-like peptide-1 (GLP-1) release, but systemic exposure causes unwanted side effects, such as gallbladder filling. In the present study, linagliptin, a DPP-4 inhibitor with a large molecular weight and polarity, and MN6, a previously described TGR5 agonist, were linked to produce OL3, a novel low-absorbed TGR5 agonist with reduced side-effects and dual function in lowering blood glucose by activation of TGR5 and inhibition of DPP-4.
Methods: TGR5 activation was assayed in HEK293 cells stably expressing human or mouse TGR5 and a CRE-driven luciferase gene. DPP-4 inhibition was assessed based on the rate of hydrolysis of a surrogate substrate. GLP-1 secretion was measured in human enteroendocrine NCI-H716 cells. OL3 permeability was tested in Caco-2 cells. Acute glucose-lowering effects of OL3 were evaluated in ICR and diabetic *ob/ob* mice.
Results: OL3 activated human and mouse TGR5 with an EC_{50} of 86.24 and 17.36 nmol/L, respectively, and stimulated GLP-1 secretion in human enteroendocrine NCI-H716 cells (3–30 μmol/L). OL3 inhibited human and mouse DPP-4 with IC_{50} values of 18.44 and 69.98 μmol/L, respectively. Low permeability of OL3 was observed in Caco-2 cells. In ICR mice treated orally with OL3 (150 mg/kg), the serum OL3 concentration was 101.10 ng/mL at 1 h, and decreased to 13.38 ng/mL at 5.5 h post dose, confirming the low absorption of OL3 *in vivo*. In ICR mice and *ob/ob* mice, oral administration of OL3 significantly lowered the blood glucose levels, which was a synergic effect of activating TGR5 that stimulated GLP-1 secretion in the intestine and inhibiting DPP-4 that cleaved GLP-1 in the plasma. In ICR mice, oral administration of OL3 did not cause gallbladder filling.
Conclusion: OL3 is a low-absorbed TGR5 agonist that lowers blood glucose without inducing gallbladder filling. This study presents a new strategy in the development of potent TGR5 agonists in treating type 2 diabetes, which target to the intestine to avoid systemic side effects.

Keywords: OL3; MN6; linagliptin; TGR5 agonist; DPP4 inhibitor; GLP-1; low-absorbed; gallbladder filling; type 2 diabetes mellitus

Acta Pharmacologica Sinica (2016) 37: 1359–1369; doi: 10.1038/aps.2016.27; published online 6 Jun 2016

Introduction

TGR5 (GPR131) was identified as a Gαs protein-coupled cell-surface receptor for bile acids (BAs) in 2002[1, 2] with broad distribution in many tissues, including the gallbladder, intestine, kidney and placenta[3, 4]. The activation of TGR5 signaling triggered by BAs leads to glucagon-like peptide-1 (GLP-1) secretion in enteroendocrine cells[5–7]. GLP-1 secretion is known to increase postprandial insulin secretion and to regulate glucose homeostasis in indirect ways, including slowing gastric motility and suppressing appetite[8, 9]. In addition, TGR5 plays a role in the enhancement of energy expenditure in skeletal muscle and brown adipose tissue via cAMP-dependent activation of type 2 iodothyronine deiodinase (D2) and the thyroid hormone pathway[10, 11]. Although these effects indicate that TGR5 is a promising target in treating metabolic disorders, potential side effects limit the development of TGR5 agonists into medications. Recent studies by Li and Lavoie *et al*[12, 13] reveal that stimulation of TGR5 by the selective agonist INT-777 relaxes smooth muscle in the gallbladder. This results in gallbladder filling and volume expansion, which is a major obstacle in the clinical application of TGR5 agonists. In addition, impaired immune responses[14] and alterations in heart rate have been identified as side effects of TGR5 activation[15, 16]. Recent research has demonstrated that TGR5 activation and subsequent GLP-1 secretion occur at the luminal

*To whom correspondence should be addressed.
E-mail jhshen@mail.shcnc.ac.cn (Jian-hua SHEN);
yleng@simm.ac.cn (Ying LENG)
Received 2016-02-02 Accepted 2016-04-05

side of the enteroendocrine L cells in the intestine, primarily in the colon. Thus, systemic exposure to a TGR5 agonist is not necessary for the modulation of glucose homeostasis[17, 18]. The development of low/non-systemic agonists of TGR5 to reduce side effects is a critical goal in type 2 diabetes treatment.

Our previous study identified a series of potent and selective small-molecule TGR5 agonists[19]. Among them, MN6 ([4-(2, 5-dichlorophenoxy) pyridin-3-yl]-(4-cyclopropyl-3,4-dihydro-2H-quinoxalin-l-yl) methanone (described as compound 22g in reference 19) is one of the most potent molecules with an EC_{50} of 1.5 nmol/L and 18 nmol/L on human and mouse TGR5 (h/mTGR5), respectively, and without activation effects on FXR[19]. Oral administration of MN6 (described as compound 2 in reference 20) also increased the gallbladder volume in mice[20]. Compounds with a large molecular weight (MW) and a high topological polar surface area (tPSA) exhibit low membrane permeability and decreased intestinal absorption[21]. Hence, MN6 incorporated with hydrophilic side chains may reduce systemic exposure and decrease side effects.

Augmentation of active form GLP-1 level can be accomplished not only by stimulating GLP-1 secretion in the intestine but also by slowing its degradation. Circulating GLP-1 has a short half-life (approximately 1–2 min) due to rapid N-terminal dipeptide cleavage into inactive metabolites by dipeptidyl peptidase-4 (DPP-4)[22–24]. This inactivation process of GLP-1 can be prevented by DPP-4 inhibitors, leading to the development of different DPP-4 inhibitors that are already used in clinical trials as monotherapy or combination therapy with other hypoglycemic agents[25]. Linagliptin is one of the most selective and potent inhibitors of DPP-4, with an IC_{50} of approximately 1 nmol/L, and was approved by the FDA in 2011. In addition, the structure of linagliptin is based on a xanthine scaffold with a large MW of 472.5 and a high tPSA[26]. To decrease the intestinal absorption of MN6, linagliptin was incorporated as a hydrophilic side chain to yield the low-systemic agent OL3. This compound was expected to generate a synergistic effect in increasing active form GLP-1 level by targeting TGR5 activation in the intestine and DPP-4 inhibition in plasma to increase GLP-1 (Figure 1).

In the present study, we designed and synthesized a novel compound, OL3, with low-systemic exposure and dual functional targeting of TGR5 activation and DPP-4 inhibition. The ability of OL3 to activate TGR5 and inhibit DPP-4 was evaluated both *in vitro* and *in vivo*. Moreover, we characterized the acute effects of OL3 on regulating glucose homeostasis in normal and diabetic mice. The effects of OL3 on gallbladder filling was observed in ICR mice.

Materials and methods

Chemicals

The synthesis of OL3 is shown in Scheme 1.

Ethyl (E)-3-(2,5-dichloro-4-((3-(4-cyclopropyl-1,2,3,4-tetrahydroquinoxaline-1-carbonyl)pyridin-4-yl)oxy)phenyl)acrylate (2)

To a solution of compound **1** (5.20 g, 10 mmol) in MeCN, ethyl acrylate (2.17 mL, 20 mmol) was added, followed by palladium diacetate (225 mg, 1.0 mmol), Tris (2-methylphenyl) phosphine (400 mg, 2.0 mmol), Et_3N (3.5 mL, 50 mmol) and lithium chloride (430 mg, 10 mmol). The resulting mixture was heated with a microwave reactor at 140 °C for 1 h. After cooling to ambient temperature, the reaction mixture was poured into water and extracted with ethyl acetate. The organic layers were combined, washed with saturated brine, dried over anhydrous magnesium sulfate, and concentrated under reduced pressure. The residue was purified by flash column chromatography to yield the title compound 4.05 g (75%). ^{1}H NMR (300 MHz, $CDCl_3$): δ 8.88 (s, 1H), 8.46 (d, 1H), 7.91 (d, 1H), 7.65 (s, 1H), 7.04–6.99 (m, 1H), 6.89 (d, 1H), 6.48 (d, 1H), 6.42–6.37 (m, 3H), 5.73 (s, 1H), 4.89 (m, 1H), 4.28 (q, 2H), 3.49 (m, 2H), 3.17 (m, 1H), 2.22 (m, 1H), 1.35 (t, 3H), 0.65 (m, 3H), 0.27 (m, 1H).

Ethyl 3-(2,5-dichloro-4-((3-(4-cyclopropyl-1,2,3,4-tetrahydroquinoxaline-1-carbonyl)pyridin-4-yl)oxy)phenyl)propanoate (3)

To a mixture of **2** (3.5 g, 6.5 mmol) and cuprous chloride (965 mg, 9.75 mmol) in methanol and tetrahydrofuran at 0 °C was added $NaBH_4$ (1.24 g, 32.5 mmol) in batches and the resulting mixture was stirred at 8 °C for 2 h. The reaction was then quenched by the addition of water. The resulting solid was filtered off, and the filtrate was concentrated under reduced

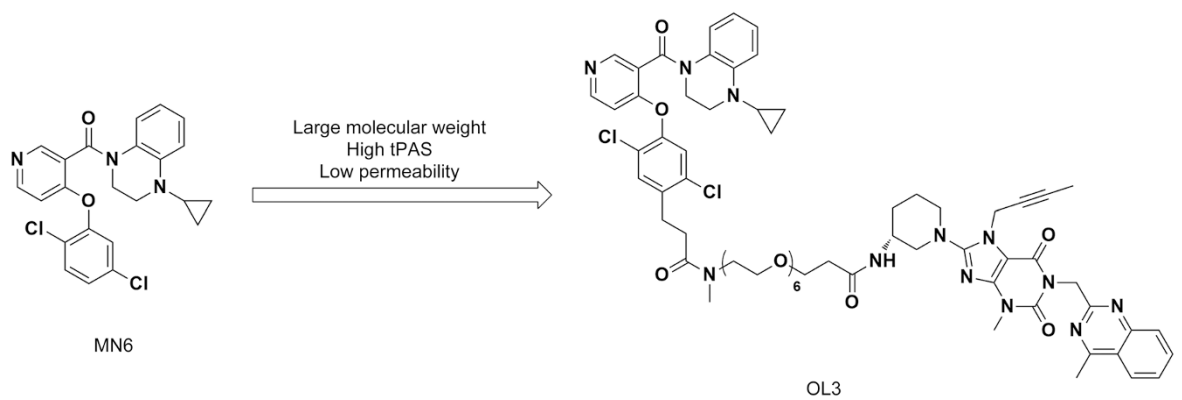

Figure 1. OL3 was designed and synthesized based on the structure of MN6.

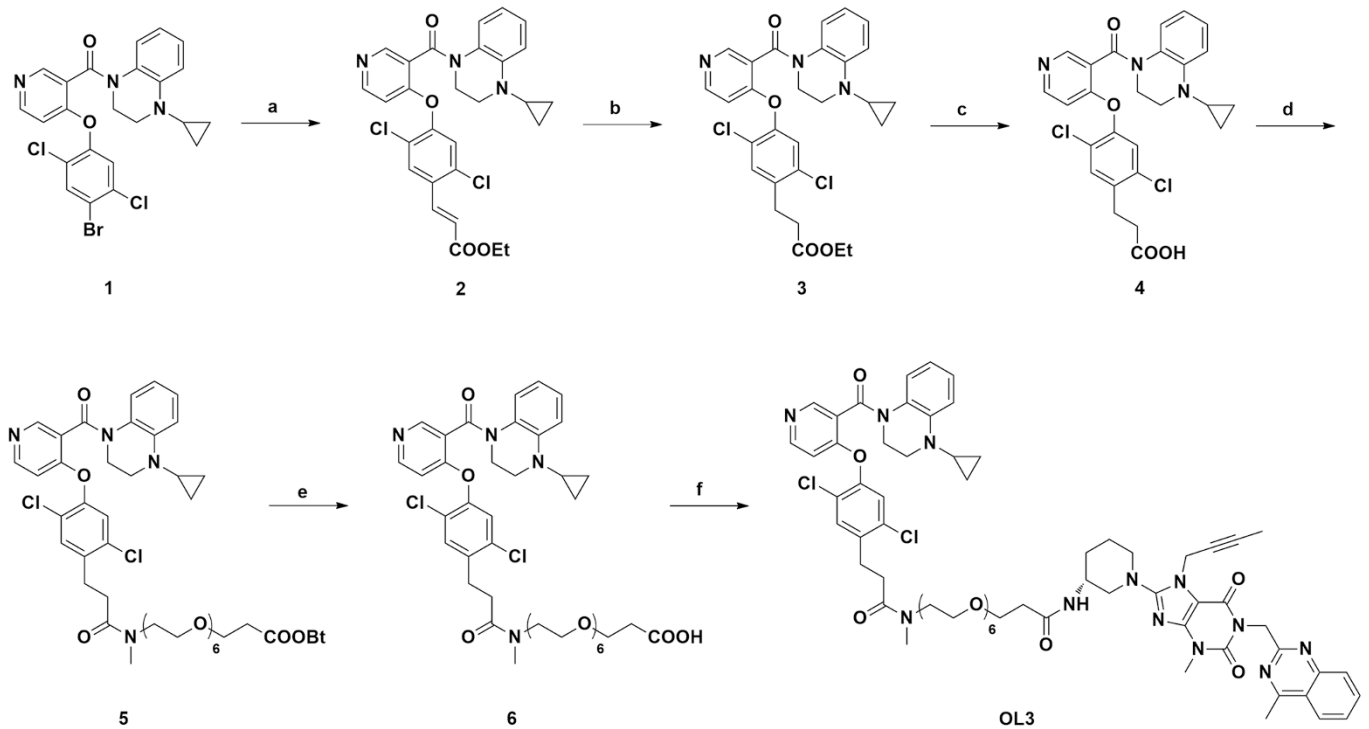

Scheme 1. Synthesis of OL3. Reagents and conditions: a) Ethylacrylate, $Pd(OAc)_2$, $P(O\text{-}MePh)_3$, LiCl, MeCN, microwave 140 °C; b) $NaBH_4$, CuCl, THF, MeOH, 0 °C; c) NaOH, dioxane, H_2O, room temperature; d) Tert-butyl-5,8,11,14,17,20-hexaoxa-2-azatricosan-23-oate, HATU, Et_3N, DCM, room temperature; e) CH_3COCl, H_2O, DCM, room temperature; f) Linagliptin, HATU, Et_3N, DCM, room temperature.

pressure. The residue was diluted with water and extracted with dichloromethane. Organic layers were combined, dried over anhydrous magnesium sulfate and evaporated under reduced pressure. The residue was purified by flash column chromatography with petroleum ether/ethyl acetate to yield 2.84 g (81%) of **3** as a yellow oil. ^{1}H NMR (300 MHz, DMSO): δ 8.82 (s, 1H), 8.40 (d, 1H), 7.30 (s, 1H), 7.03 (m, 1H), 6.93 (d, 1H), 6.48 (d, 1H), 6.37 (m, 1H), 6.29 (d, 1H), 5.69 (s, 1H), 4.89 (m, 1H), 4.15 (q, 2H), 3.49 (m, 2H), 3.17 (m, 1H), 2.99 (t, 2H), 2.61 (t, 2H), 2.25 (m, 1H), 1.26 (t, 3H), 0.62 (m, 3H), 0.34 (m, 1H).

3-(2,5-dichloro-4-((3-(4-cyclopropyl-1,2,3,4-tetrahydroquinoxaline-1-carbonyl)pyridin-4-yl)oxy)phenyl)propanoic acid (4)

To a solution of **3** (2.7 g, 5.0 mmol) in 1,4-dioxane and water was added sodium hydroxide (0.40 g, 10 mmol) and the reaction mixture was stirred at ambient temperature for 3 h. The reaction was evaporated to dryness, and the residue was dissolved in water. The pH of the solution was adjusted to 3 with 2 mol/L HCl. The formed precipitate was filtered, washed with cold water, and dried under vacuum to yield the title compound 2.36 g (92%). ^{1}H NMR (300 MHz, DMSO): δ 12.29 (s, 1H), 8.77 (s, 1H), 8.41 (d, 1H), 7.59 (s, 1H), 6.97 (m, 1H), 6.84 (m, 1H), 6.53 (m, 1H), 6.48 (m, 1H), 6.33 (m, 1H), 5.54 (s, 1H), 4.71 (m, 1H), 3.36 (m, 2H), 3.07 (m, 1H), 2.86 (m, 2H), 2.51 (m, 1H), 2.16 (m, 1H), 0.60 (m, 2H), 0.47 (m, 1H), 0.44 (m, 1H).

Tert-butyl 1-(2,5-dichloro-4-((3-(4-cyclopropyl-1,2,3,4-tetrahydroquinoxaline-1-carbonyl)pyridin-4-yl)oxy)phenyl)-4-methyl-3-oxo-7,10,13,16,19,22-hexaoxa-4-azapentacosan-25-oate (5)

To a solution of **4** (1 mmol) in dichloromethane was added HATU (1.5 mmol), followed by Et_3N (3 mmol) and tert-butyl 5,8,11,14,17,20-hexaoxa-2-azatricosan-23-oate (1.5 mmol). The resulting mixture was stirred at room temperature overnight. The reaction mixture was diluted with water and extracted with dichloromethane. The organic layer was washed with saturated brine, dried over anhydrous magnesium sulfate, and concentrated under reduced pressure. The residue was purified by flash chromatography to yield the desired compound. ^{1}H NMR (300 MHz, $CDCl_3$): δ 8.80 (s, 1H), 8.40 (d, 1H), 7.34 (s, 1H), 7.03 (m, 1H), 6.96 (m, 1H), 6.48 (m, 1H), 6.36 (m, 1H), 6.29 (d, 1H), 5.73 (m, 1H), 4.86 (m, 1H), 3.63–3.46 (m, 30H), 3.20 (m, 1H), 3.05–2.96 (m, 5H), 2.65 (m, 1H), 2.56 (m, 1H), 2.26 (m, 1H), 1.43 (s, 9H), 0.64 (m, 3H), 0.24 (m, 1H).

1-(2,5-dichloro-4-((3-(4-cyclopropyl-1,2,3,4-tetrahydroquinoxaline-1-carbonyl)pyridin-4-yl)oxy)phenyl)-4-methyl-3-oxo-7,10,13,16,19,22-hexaoxa-4-azapentacosan-25-oic acid (6)

To a solution of 5 (1 mmol) in dichloromethane was added acetyl chloride (470 μL, 6.6 mmol) and H_2O (118 μL, 6.6 mmol). The resulting mixture was stirred at room temperature for 3 h. The reaction solution was evaporated under reduced pressure directly, purified by semi-preparative HPLC to afford the

product 105 mg. ^{1}H NMR (300 MHz, $CDCl_3$): δ 8.95(s, 1H), 8.74 (m, 1H), 7.43 (s, 1H), 7.11 (m, 2H), 6.68 (m, 1H), 6.46 (m, 2H), 5.92 (s, 1H), 4.80 (m, 1H), 3.76–3.51 (m, 29H), 3.09–2.98 (m, 5H), 2.75–2.58 (m, 4H), 2.32 (m, 1H), 0.74 (m, 3H), 0.17 (m, 1H).

(*R*)-N-(1-(7-(but-2-yn-1-yl)-3-methyl-1-((4-methylquinazolin-2-yl)methyl)-2,6-dioxo-2,3,6,7-tetrahydro-1H-purin-8-yl)piperidin-3-yl)-1-(3-(2,5-dichloro-4-((3-(4-cyclopropyl-1,2,3,4-tetrahydroquinoxaline-1-carbonyl)pyridin-4-yl)oxy)phenyl)-N-methylpropanamido)-3,6,9,12,15,18-hexaoxahenicosan-21-amide (OL3)

OL3 was synthesized from **6** by the same method as the preparation of **4** except for the replacement of 5,8,11,14,17,20-hexaoxa-2-azatricosan-23-oate with linagliptin. ^{1}H NMR (300 MHz, $CDCl_3$): δ 8.80 (s, 1H), 8.40 (d, 1H), 8.01 (d, 1H), 7.87 (d, 1H), 7.75 (d, 1H), 7.52 (d, 1H), 7.33 (s, 1H), 7.03 (m, 2H), 6.97 (m, 1H), 6.48 (m, 1H), 6.37 (m, 1H), 6.29 (m, 1H), 5.74 (m, 1H), 5.55 (s, 2H), 4.90 (m, 3H), 4.17 (m, 1H), 3.74 (t, 2H), 3.62–3.15 (m, 30H), 3.04–2.96 (m, 5H), 2.88 (s, 3H), 2.66 (m, 1H), 2.58 (m, 1H), 2.48 (t, 2H), 2.26 (m, 1H), 1.91–1.65 (m, 11H), 0.64 (m, 3H), 0.24 (m, 1H).

Animals

Male ICR mice were purchased from SLAC Laboratory Animals (Shanghai, China). B6.V-*Lep^{ob}/Lep^{ob}* mice (Jackson Laboratory, Bar Harbor, ME, USA) were bred at the Shanghai Institute of Materia Medica, Chinese Academy of Sciences (Shanghai, China). All animals were housed in environmentally controlled conditions with a 12 h light-dark cycle and free access to water and food. Animal experiments were approved by the Animal Care and Use Committee, Shanghai Institute of Materia Medica.

In vitro TGR5 activity assay

HEK293 cells stably expressing human or mouse TGR5 and the CRE-driven luciferase gene were obtained and maintained as described[27]. Briefly, HEK293 cells stably transfected with the h/mTGR5 expression plasmid (hTGR5-pcDNA3.1 or mTGR5-pcDNA3.1) and the CRE-driven luciferase reporter plasmid (pGL4.29, Promega, Madison, WI, USA) were seeded into 96-well plates and incubated in DMEM containing 10% FBS in 5% CO_2 at 37 °C overnight. Cells were then incubated in fresh medium containing different concentrations of OL3 or MN6 for 5.5 h, and activity was assessed by a reporter gene assay. Luciferase activity in the cell lysate was determined by the Steady-Glo® Luciferase Assay System (Promega, Madison, WI, USA) according to the instructions from the manufacturer.

In vitro DPP-4 activity assay

Inhibitory effects of compounds on human and mouse DPP-4 were determined by measuring the rates of Gly-Pro-7-amido-4-methylcoumarin hydrobromide (Gly-Pro-7-AMC, Sigma-Aldrich, MO, USA) hydrolysis as previously described[28]. Briefly, recombinant human DPP-4 (Enzo Life Sciences, Farmingdale, NY, USA) in 50 mmol/L Tris (pH 7.5) was incubated with different concentrations of compounds for 5 min. Then, Gly-Pro-7-AMC was added to a final concentration of 10 μmol/L, followed by monitoring of the catalysis rate to calculate the inhibitory effect of compounds. The procedures of the *in vitro* mouse DPP-4 activity assay were the same as the human DPP-4 activity assay, but the enzyme was replaced by serum from ICR mice and the buffer was changed to 25 mmol/L HEPES, 140 mmol/L NaCl, 1% BSA (pH 7.8).

GLP-1 secretion assay in NCI-H716 cells

Human enteroendocrine NCI-H716 cells were maintained in a suspension culture as described by American Type Culture Collection (ATCC, Manassas, VA, USA). Briefly, cells were seeded into 24-well plates coated with Matrigel (BD Biosciences, Oxford, UK) for 48 h. After washing with KREBS, cells were incubated with OL3, vehicle control or PMA as the positive control diluted in KREBS (with 0.2% BSA and 1% DPP-4 inhibitor) for 2 h at 37 °C. Then, samples were collected and centrifuged to remove floating cells. The active GLP-1 level was assayed using an ELISA kit from Merck-Millipore (Boston, MA, USA).

Permeability assay in Caco-2 cells

The permeability of OL3 was tested in the Caco-2 cell monolayer model, which was obtained from ATCC. Compounds transported from the apical side to the basolateral side (A–B) and from the basolateral side to the apical side (B–A) were determined under the same conditions. Propranolol and atenolol were used as the hypertonic and hypotonic controls, respectively. Digoxin was used for P-glycoprotein (P-gp)-mediated drug efflux as the positive control. Briefly, cells were seeded into 24-well plates and incubated in DMEM containing 10% FBS, 1% nonessential amino acids, 1% glutamine, 100 mg/mL streptomycin and 100 U/mL penicillin, in 5% CO_2 at 37 °C for 21 d. After washing with HBSS three times, the integrity of the monolayer was verified by the measurement of TEER (trans epithelial electric resistance). The cell monolayer was then incubated with each indicated compound diluted in HBSS (400 μL/well on apical side and 800 μL/well on basolateral side) for 90 min at 37 °C. Samples were collected from the donor side and the receiver side after incubation. The concentration of compounds was measured by LC-MS/MS. The P_{app} value was calculated using the following equation:

$$P_{app}=(V_A/(A\times T))\times([Comp]_{acceptor}/[Comp]_{initial\ donor})$$

where V_A is the acceptor well volume; A is the surface area of the membrane (cm^2); T is the time of total transport; $[Comp]_{acceptor}$ is the concentration of compound at the acceptor side, and $[Comp]_{initial\ donor}$ is the initial concentration of compound at the donor side.

Compound preparation for the *in vivo* study

Because OL3 exhibited low aqueous solubility due to a high molecular weight, the compound was prepared by combination with polyvinylpyrrolidone (PVP) K30 (Sinopharm Chemical Reagent Co, Ltd, Shanghai, China), which has been shown to improve the aqueous solubility of drugs. Briefly, 1 g of OL3 was dissolved in 50 mL of dichloromethane. Then, 5 g PVP

K30 was added, and the mixture was evaporated to produce a white powder using a vacuum. For *in vivo* experiments, the powder containing a mixture of the test compound and PVP K30 was suspended in distilled water, and the same amount of PVP K30 was used as vehicle control.

Measurement of compound levels in the serum of ICR mice

Overnight-fasted male ICR mice were randomly assigned to 4 groups (n=4 in each group). One group was orally administered the vehicle, and blood samples were collected as blank controls (0 h) for compound measurements. The other three groups were orally administered OL3 at 150 mg/kg, and blood samples were collected at 1, 3.5, and 5.5 h post administration for OL3 and linagliptin measurements. Briefly, proteins in the serum were precipitated with acetonitrile, and the supernatant was injected into the LC-MS/MS system for further quantification. Chromatographic separation was performed on a Luna C_{18} column (50 mm×2.1 mm ID for OL3 and 100 mm×2.1 mm ID for linagliptin, 1.7 μm, Waters, MA, USA) using 5 mmol/L ammonium acetate and acetonitrile (1:1, *v*/*v*) containing 0.1% formic acid as the mobile phase, which was delivered at a flow rate of 0.5 mL/min. MS detection was carried out in multiple reactions monitoring mode using a positive electrospray ionization interface. The calibration curve was established from 3.0 to 1000 ng/mL for OL3 and from 0.01 to 3 ng/mL for linagliptin.

Oral glucose tolerance test (OGTT) and gallbladder volume measurement in ICR mice

ICR mice were divided into 5 groups (n=8 in each group) based on fasting blood glucose level and body weight. Overnight-fasted ICR mice were orally dosed with 75, 150, or 300 mg/kg OL3, 50 mg/kg MN6 or vehicle, followed by an oral bolus of 4 g/kg glucose 90 min later. Blood was obtained by clipping the tail, and glucose levels were measured with an ACCU-CHEK Advantage II Glucose Monitor (Roche, IN, USA) at 15 min prior to the compound dose and at 0, 15, 30, 60, and 120 min post glucose dose. The area under the concentration-time curve from 0 to 120 min ($AUC_{0-120\ min}$) of blood glucose after glucose loading was determined by the trapezoidal rule (using the 0 time glucose level for each animal as that animal's baseline). After the OGTT, the mice were provided food for 2 h. The mice were then sacrificed and dissected, and the volume of the gallbladder was measured using a vernier caliper. The relative volume of the gallbladder was calculated by the length multiplied by the width of the gallbladder.

Fasting-blood glucose level measurement in diabetic *ob/ob* mice

Female *ob/ob* mice were assigned to 3 groups (n=7–8 in each group) based on blood glucose level and body weight. Two-hour-fasted *ob/ob* mice were orally administered vehicle or OL3 at 200 or 400 mg/kg. Blood was obtained by clipping the tail, and glucose levels were measured at 0, 2, 4 h after the compound dose with an ACCU-CHEK Advantage II Glucose Monitor.

Oral glucose tolerance test (OGTT) in diabetic *ob/ob* mice

Female *ob/ob* mice were assigned to 3 groups (n=7–8 in each group) based on the fasting blood glucose level and body weight. Five-hour-fasted *ob/ob* mice were orally administered the vehicle or OL3 at 200 or 400 mg/kg, followed by an oral bolus of 1.5 g/kg glucose at 90 min post compound dose. At 0, 15, 30, 60, and 120 min post glucose loading, blood samples were collected from the retroorbital sinus, and the serum glucose level was determined with a glucose oxidase-peroxidase method using a Glucose Assay Kit (Rongsheng Biotech, Shanghai, China).

In vivo DPP-4 inhibition in ICR mice

This experiment was performed simultaneously with OGTT in ICR mice. Briefly, overnight-fasted ICR mice were orally dosed with OL3, MN6 or vehicle, and blood samples were collected at 0, 1, 3.5, 5.5 h later. Serum DPP-4 activity was measured at the same with the *in vitro* mouse DPP-4 inhibition assay but addition of the compounds was omitted.

Effects of OL3 on the active form of GLP-1 in plasma in ICR mice

ICR mice were assigned to 2 groups (n=30 in each group) based on body weight. The effect of OL3 on the active form of GLP-1 in plasma was evaluated under basal and glucose-stimulated conditions. For the basal group, mice were fasted for 6 h, followed by oral administration of OL3 (150 mg/kg), linagliptin (0.1 mg/kg) or the vehicle (n=10). Blood samples were collected at 1.5 h post compound dose. In the glucose-stimulated group, mice were overnight-fasted, followed by oral treatment with OL3 (150 mg/kg), linagliptin (0.1 mg/kg) or vehicle (n=10). At 1.5 h post compound dose, all mice were challenged with 4 g/kg oral glucose, and blood samples were collected 5 min after glucose loading. All blood samples were placed in Eppendorf tubes containing the DPP-IV inhibitor (Merck-Millipore, Boston, MA, USA), with a final concentration of 1% blood samples and 25 mg/mL EDTA. The active form of GLP-1 in plasma was quantified using an ELISA kit (Merck-Millipore, Boston, MA, USA). Serum DPP-4 activity in glucose-stimulated mice was also determined.

Statistical analysis

Statistical calculations were performed using the GraphPad Prism 5 program (GraphPad Software, San Diego, CA, USA). The results are expressed as the mean±SEM. All statistical analyses were performed with a two-tailed unpaired t test. Difference was considered significant at P<0.05.

Results

Chemistry

The synthesis of OL3 is outlined in Scheme 1. The starting material 1, synthesized as previously reported[19], was coupled to ethylacrylate by a microwave-assisted Pd catalyzed Heck reaction, followed by reduction and hydrolysis to yield the key intermediate 4. Condensation of the acid 4 with tert-butyl-5,8,11,14,17,20-hexaoxa-2-azatricosan-23-oate gave the ester 5

using HATU as condensation agent. Hydrolysis of the esters 5 yielded the compound 6 which underwent condensation with linagliptin in the same condition to yield the target compound OL3 (Scheme 1).

OL3 is a potent TGR5 agonist with a weak inhibitory effect on DPP-4 *in vitro*

As shown in Figure 2A and 2B, OL3 exhibited potent activity with EC_{50} values of 86.24 nmol/L on hTGR5 and 17.36 nmol/L on mTGR5. INT-777, which has been widely used as a TGR5 agonist to investigate TGR5 physiological functions, exhibited EC_{50} values of 1.08 μmol/L and 0.35 μmol/L on hTGR5 and mTGR5, respectively, which were consistent with previous reports[29]. Because OL3 contained the DPP-4 inhibitor group linagliptin, we investigated the inhibitory effect of OL3 on DPP-4. A weak inhibitory effect was observed for OL3 at a high concentration with an IC_{50} value of approximately of 18.44 and 69.98 μmol/L against human and mouse DPP-4 (h/mDPP-4), respectively. As a positive control, linagliptin demonstrated an IC_{50} of 1.00 nmol/L and 2.91 nmol/L against hDPP-4 and mDPP-4, respectively (Figure 3), as previously reported[30]. These results indicated that OL3 exerted dual functions in potently activating TGR5 and weakly inhibiting DPP-4 *in vitro*.

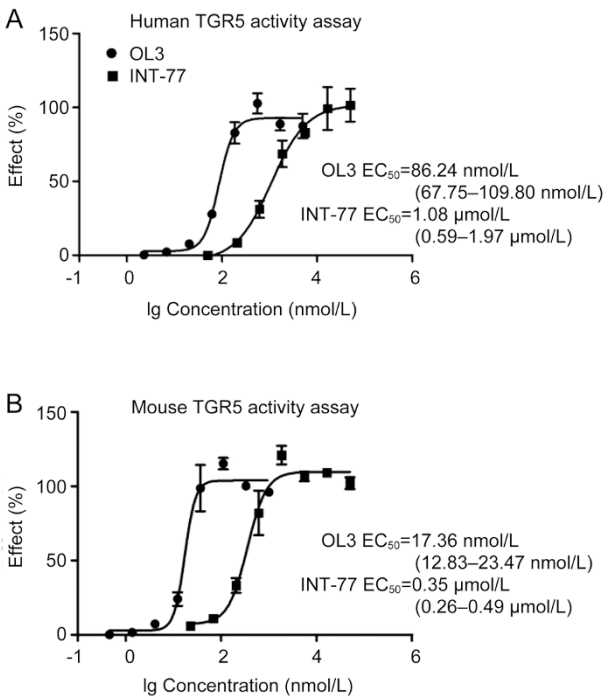

Figure 2. The activation effects of OL3 on human and mouse TGR5 *in vitro*. Compounds were tested for their potency on TGR5 activation in HEK293 cells transfected with the hTGR5 (A) or mTGR5 (B) expression plasmids and the CRE-Luc reporter gene plasmid. The 95% confidence limits of the EC_{50} values for each compound were calculated based on data obtained from three independent experiments.

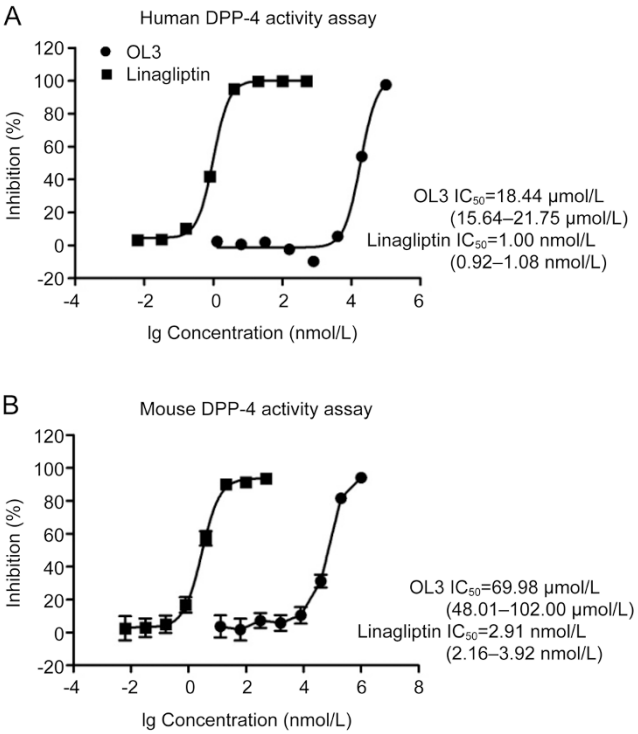

Figure 3. The inhibition effects of OL3 and linagliptin on human and mouse DPP-4 activity *in vitro*. The inhibitory effects of compounds on human recombinant DPP-4 (A) or mouse serum DPP-4 (B) were calculated against the vehicle control. The 95% confidence limits of the IC_{50} values for each compound were calculated based on data obtained from three independent experiments.

OL3 dose-dependently stimulated GLP-1 secretion in NCI-H716 cells

To determine the potency of OL3 in stimulating GLP-1 secretion *in vitro*, NCI-H716 cells (a human enteroendocrine L cell line) endogenously expressing TGR5[7, 31, 32] were employed. Phorbol 12-myristate 13-acetate (PMA) served as a positive control. The results demonstrated that OL3 robustly increased GLP-1 secretion in a dose-dependent manner. A 2-h incubation of OL3 at 3 μmol/L resulted in a 1.5-fold increase in GLP-1 secretion. A maximum increase of 2.4-fold was achieved after exposure to 30 μmol/L OL3 (Figure 4), confirming that OL3 induced GLP-1 secretion in enteroendocrine cells *in vitro*.

OL3 demonstrated low permeability in Caco-2 cells

The human colon carcinoma (Caco-2) cell is widely used to characterize intestinal absorption and secretion of drugs *in vitro*[33]. MN6 demonstrated a high permeability in Caco-2 cells in our previous report (P_{app}=6.75×10^{-6} cm/s)[20]. In the current study, Caco-2 cells were used to evaluate the permeability of OL3 *in vitro*. As expected, the Caco-2 permeability of OL3 (P_{app}=0.03×10^{-6} cm/s) was much lower than that of MN6 and another positive control, propranolol (P_{app}=19.20×10^{-6} cm/s), implying that OL3 is a hypo-osmosis agent compared with MN6 (Table 1).

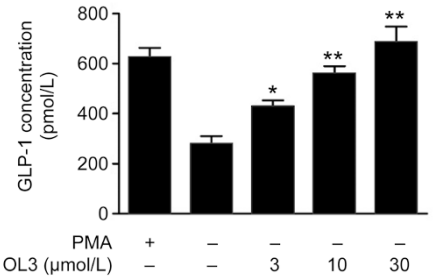

Figure 4. OL3 dose-dependently stimulated GLP-1 secretion in NCI-H716 cells. NCI-H716 cells were treated with 1 μmol/L PMA or OL3 at indicated concentrations for 2 h, and expression of the active form of GLP-1 level was measured (n=3). The results are presented as the mean±SEM. $^{*}P$<0.05, $^{**}P$<0.01 *vs* control treatment.

Table 1. Apparent permeability of OL3 in Caco-2 cells.

Compd	P_{app} (10^{-6} cm/s)		Efflux r
	A to B	B to A	
Propranolol	19.20	12.90	–
Atenolol	0.10	0.60	–
Digoxin	0.10	15.80	153.00
OL3	0.03	13.58	461.00

P_{app} level of A to B was P_{app} level of compounds transported from the apical side to the basolateral side; P_{app} level of B to A was P_{app} level of compounds transported from the basolateral side to the apical side.

Pharmacokinetic studies in ICR mice

Because OL3 exhibited low permeability in the Caco-2 model, we performed pharmacokinetic studies in ICR mice to further investigate its absorption *in vivo*. After an oral administration of OL3 at 150 mg/kg to ICR mice, the concentration of OL3 in the serum was examined at 1.0, 3.5, 5.5 h post dose. As shown in Table 2, the concentration of OL3 reached 101.10 ng/mL at 1 h, and then decreased to 13.38 ng/mL at 5.5 h post dose, confirming the low absorption of OL3 *in vivo*. The serum concentration of linagliptin was 0.19, 0.16, 0.06 ng/mL at 1.0, 3.5, 5.5 h post dose, respectively. These data indicated that OL3 was poorly absorbed and thus exhibited low systemic exposure *in vivo*; as one of the OL3 metabolites, linagliptin was also detected in the serum.

Table 2. Levels of OL3 and linagliptin in serum after oral administration of 150 mg/kg OL3 to ICR mice. Data were mean±SEM of 4 mice.

Time	OL3 (ng/mL)	Linagliptin (ng/mL)
0 h	BLQ	BLQ
1.0 h	101.10±24.80	0.19±0.01
3.5 h	43.10±4.21	0.16±0.03
5.5 h	13.38±7.48	0.06±0.02

BLQ: Below limit quantification.

Acute administration of OL3 to ICR mice improved glucose tolerance without inducing gallbladder filling

To evaluate the *in vivo* effect of OL3 on glucose homeostasis, OGTT was performed in ICR mice. As shown in Figure 5A, the blood glucose level increased and reached a peak value at 30 min after glucose challenge. Administration of OL3 at doses of 75, 150, 300 mg/kg significantly reduced blood glucose peak values by 21.72%, 27.54%, and 30.76% (13.96±0.70

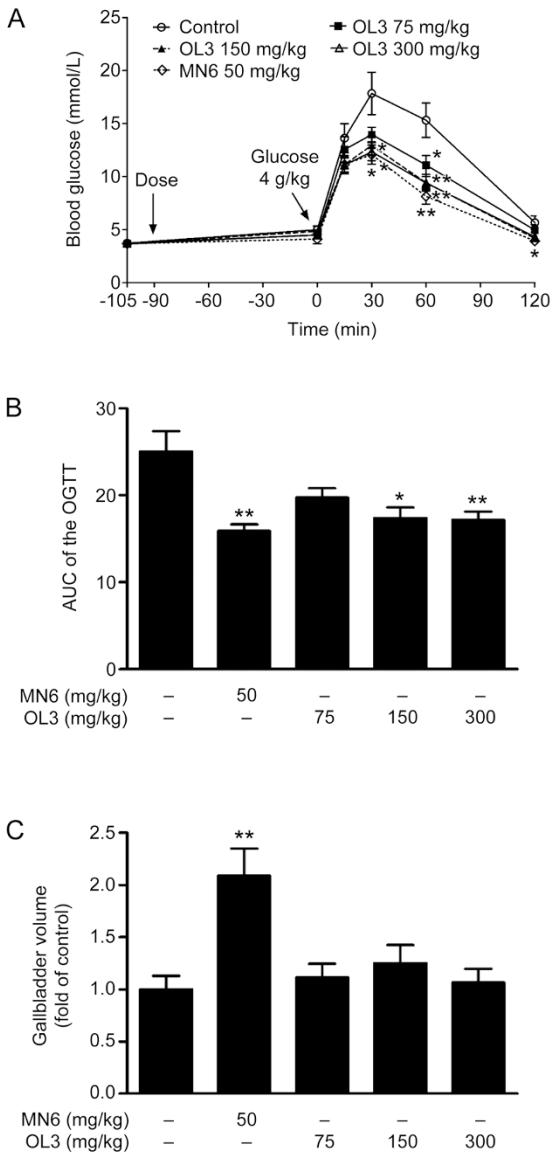

Figure 5. OL3 improved oral glucose tolerance without obvious gallbladder filling in ICR mice. Male ICR mice (n=8) were orally administered OL3 or MN6 at indicated concentrations or vehicle controls 90 min prior to 4 g/kg oral glucose loading for OGTT experiment. (A) Blood glucose levels were tested at indicated time points, and (B) the area under the curve (AUC) was calculated. After the OGTT experiment, fasting mice were provided food for 2 h, and gallbladder volume was measured (C). The results are presented as the mean±SEM. $^{*}P$<0.05, $^{**}P$<0.01 in comparison to the control group.

mmol/L, 12.93±0.89 mmol/L, 12.35±0.85 mmol/L in 75, 150, 300 mg/kg OL3 groups, respectively, *vs* 17.84±2.00 mmol/L in the control group), respectively, compared to 32.31% by 50 mg/kg MN6 (12.08±0.90 mmol/L in the MN6 group *vs* 17.84±2.00 mmol/L in the control group). A dose-dependent reduction in the $(AUC)_{0-120\ min}$ of blood glucose was observed, and 300 mg/kg of OL3 exhibited a maximum reduction of 31.43% compared with the control group. MN6 at a concentration of 50 mg/kg exhibited a reduction of 36.52% (17.17±0.98 mmol/L·h in the 300 mg/kg OL3 group, 15.89±0.76 mmol/L·h in the MN6 group *vs* 25.03±2.33 mmol/L·h in the control group, Figure 5B). At the end of the OGTT, the mice were provided food for 2 h, and gallbladder filling was assessed by measuring its volume. A 2.09-fold increase in the gallbladder volume was observed in mice treated with MN6 at a dose of 50 mg/kg, while OL3 did not induce any significant increase in volume compared with the control group (Figure 5C). These results indicate that OL3 improved glucose tolerance without significantly inducing gallbladder filling in ICR mice.

OL3 decreased fasting blood glucose level and improved oral glucose tolerance in diabetic *ob/ob* mice

As one of the most widely used metabolic abnormal animal models, genetic type 2 diabetic *ob/ob* mice demonstrate hyperglycemia and impaired glucose tolerance in response to oral glucose challenge. A single oral administration of OL3 at 200 mg/kg led to a significant decrease in the fasting blood glucose level by 24.65% (13.27±1.19 mmol/L in the 200 mg/kg OL3 group *vs* 17.61±1.44 mmol/L in the control group) 2 h post dose; 400 mg/kg of OL3 further significantly decreased the fasting blood glucose level by 24.73% and 22.98% at 2 h and 4 h post dose, respectively, (13.26±1.10 mmol/L and 15.53±1.59 mmol/L in 2 h and 4 h of the 400 mg/kg OL3 group, respectively, *vs* 17.61±1.44 mmol/L and 20.16±1.25 mmol/L in 2 h and 4 h of the control group, respectively, Figure 6A). A single oral treatment of OL3 at 400 mg/kg also improved the glucose tolerance of *ob/ob* mice, leading to a significant reduction in blood glucose by 14.11% and 12.64% at 15 and 30 min post glucose challenge, respectively, (35.65±1.56 mmol/L and 40.69±2.17 mmol/L in 15 and 30 min of the 400 mg/kg OL3 group, respectively, *vs* 41.50±0.95 mmol/L and 46.58±1.33 mmol/L in 15 and 30 min of the control group, respectively, Figure 6B) and demonstrated a tendency to reduce the $(AUC)_{0-120\ min}$ of blood glucose (Figure 6C). These results demonstrated that OL3 could improve glucose homeostasis in diabetic *ob/ob* mice.

The improvement of glucose homeostasis by OL3 was a synergistic effect of stimulating GLP-1 secretion in the intestine and inhibiting GLP-1 degradation in the plasma.

Given that OL3 exhibited dual functions in activating TGR5 and inhibiting DPP-4 *in vitro*, we further investigated whether OL3 exhibited the same synergistic mechanisms in lowering glucose *in vivo*. As shown in Figure 7A, at 1 h post-dose, 75 mg/kg, 150 mg/kg and 300 mg/kg of OL3 reduced DPP-4 activity in serum by 25.34%, 26.17% and 26.24%, respectively.

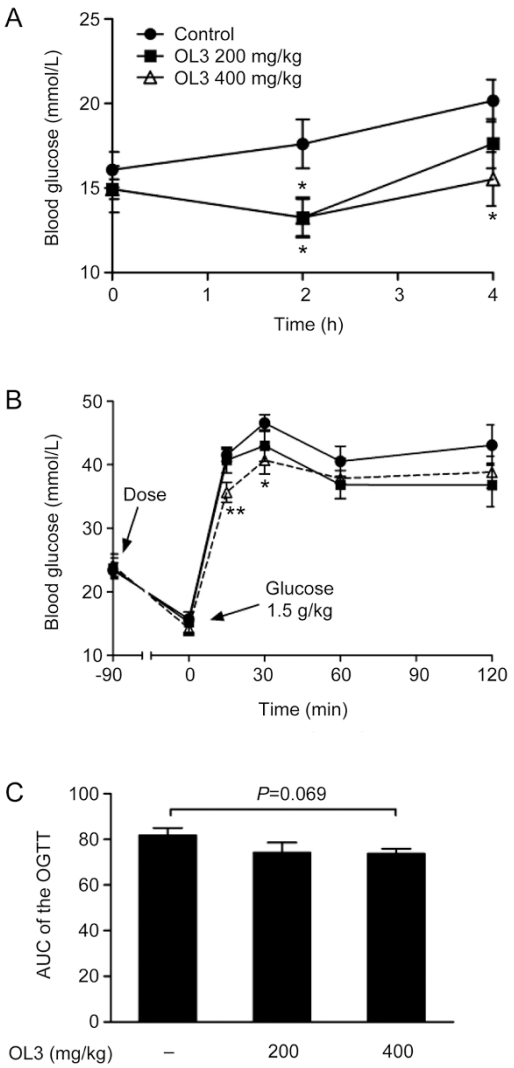

Figure 6. OL3 decreased blood glucose level and improved oral glucose tolerance in diabetic *ob/ob* mice. (A) The blood glucose level was determined after a single oral treatment of OL3 at 200 and 400 mg/kg or vehicle control to 2 h-fasting female *ob/ob* mice (n=7–8) at indicated time points. Female *ob/ob* mice (n=7–8) were administered OL3 at indicated concentration or vehicle control at 90 min prior of 1.5 g/kg glucose loading for OGTT experiment. (B) Blood glucose levels were tested, and (C) the area under the curve (AUC) was calculated. The results are presented as the mean±SEM. $^{*}P<0.05$ in comparison with the control treatment.

OL3 at 150 mg/kg and 300 mg/kg maintained the intensity of inhibition throughout the experiment, while a single dose of MN6 at 50 mg/kg showed no DPP-4 inhibitory efficacy. We further investigated the effects of OL3 on TGR5 activation *in vivo*. As shown in Figure 7B, 0.1 mg/kg linagliptin reduced DPP-4 activity by 38.72%, which was comparable to effects of 150 mg/kg OL3 (a reduction of 35.15%). Hence, 0.1 mg/kg linagliptin was set as a control to mimic the inhibitory effect of 150 mg/kg OL3 on DPP-4 activity. We quantified the active form of GLP-1 in plasma after administration of 150 mg/kg OL3 or 0.1 mg/kg linagliptin under basal or glucose-stimulated conditions. The results revealed that under basal condi-

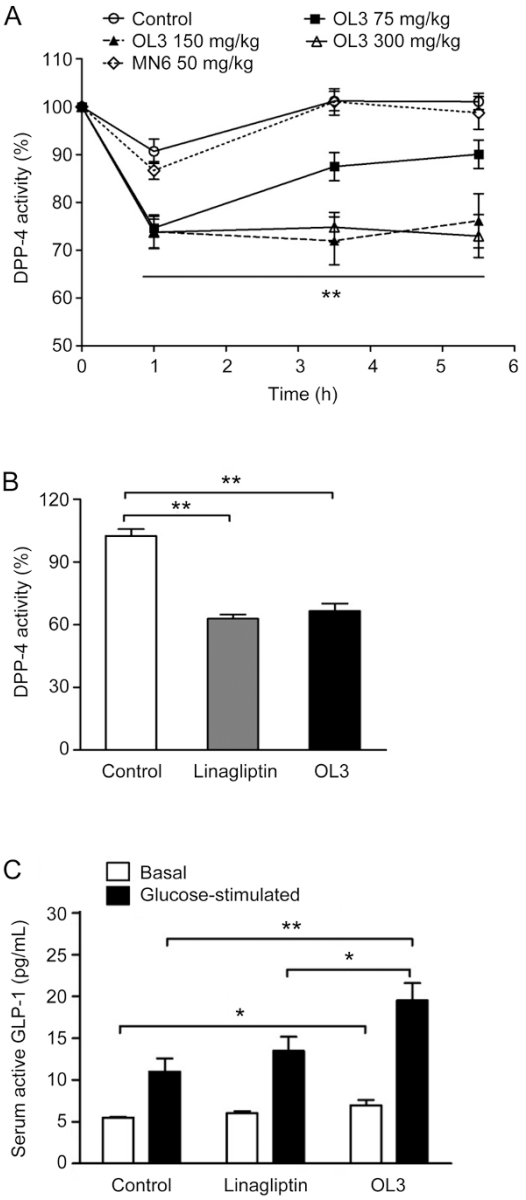

Figure 7. The impact of OL3 on glucose homeostasis resulted from a synergistic effect of stimulating GLP-1 secretion in the intestine and inhibiting GLP-1 degradation in plasma. (A) Serum DPP-4 activity was measured at indicated time points after oral administration of OL3 at 75, 150, and 300 mg/kg doses, MN6 at a dose of 50 mg/kg or vehicle to ICR mice (n=8). (B) 6 h-fasted (basal group) or overnight-fasted (glucose-stimulated group) ICR mice (n=10) were administered OL3 150 mg/kg, linagliptin 0.1 mg/kg or vehicle control, and overnight-fasted mice were further challenged with 4 g/kg glucose at 1.5 h post dose. Serum DPP-4 activity was evaluated in mice challenged with glucose. (C) Expression of the active form of GLP-1 in plasma was determined under both basal and glucose stimulated conditions. The results are presented as the mean±SEM. $^{*}P$<0.05, $^{**}P$<0.01 as compared to the control treatment as indicated.

tions, OL3 led to a significant increase of 26.44% compared with the control group and displayed a tendency to increase the active form of GLP-1 in plasma compared to linagliptin. Under the glucose-stimulated conditions, OL3 was associated with increased active form of GLP-1 by 44.89% compared to linagliptin (Figure 7C), indicating that in addition to inhibiting DPP-4 activity, OL3 also increased the secretion of GLP-1 by activating TGR5. These data suggested that increased active form of GLP-1 in plasma stimulated by OL3 was the result of a synergistic effect of stimulating secretion and inhibiting degradation.

Discussion

TGR5 has been identified as a promising target for type 2 diabetes treatment by promoting GLP-1 secretion in intestinal L cells and regulating energy expenditure in muscle and brown adipose tissue[34]. However, the development of TGR5 agonists was stalled due to the presence of unwanted systemic side effects[35]. In the current study, for the first time, we combined linagliptin, a DPP-4 inhibitor with a large polarity[36], with MN6, a novel TGR5 agonist, to generate the novel low-systemic exposure agent OL3. Moreover, we characterized OL3 as a novel potent TGR5 agonist that significantly increased the active form of GLP-1 in plasma and lowered blood glucose levels without causing gallbladder filling in mice.

In our previous study, MN6 had been characterized as a potent TGR5 agonist with an EC_{50} of 1.5 nmol/L and 18 nmol/L on human and mouse TGR5, respectively[19]. OL3 was generated by combining linagliptin with MN6. The *in vitro* assay confirmed that OL3 maintained a satisfactory activation potency with EC_{50} values of 86.24 nmol/L and 17.36 nmol/L on human and mouse TGR5, respectively. Moreover, OL3 dose-dependently stimulated GLP-1 secretion in NCI-H716 cells endogenously expressing TGR5, further confirming that OL3 activates TGR5 *in vitro*. Meanwhile, OL3 also demonstrated weak inhibition of human and mouse DPP-4 *in vitro*, which could be due to the incorporation of linagliptin. To evaluate the intestinal absorption of OL3, a permeability assay was performed on a Caco-2 monolayer, which is a widely accepted cell model for investigating the absorption and secretion of medications in the intestine[33, 37]. As expected, the addition of the linagliptin group was associated with a much lower permeability of OL3 compared to MN6. The *in vivo* pharmacokinetic study of OL3 was also performed in ICR mice. Serum concentrations of OL3 were 101.10, 43.10 and 13.38 ng/mL at 1.0, 3.5 and 5.5 h after oral administration of a 150 mg/kg dose of OL3. In our previous study, we reported the *in vivo* absorption of an analogue of MN6, described as compound 23g. Administration of 50 mg/kg of 23g to ICR mice resulted in serum concentrations of 1243 ng/mL and 936 ng/mL at 0.5 h and 1 h post dose, respectively[19], which further suggested that OL3 is a low-systemic exposure agent. Therefore, by introducing linagliptin to MN6, we generated a novel compound with strong TGR5 agonistic and weak DPP-4 inhibitory activity, but low permeability *in vitro* and low-systemic exposure *in vivo*.

The acute effects of OL3 on lowering glucose were studied in normal and type 2 diabetic animal models. A single oral dose of OL3 at 75, 150, or 300 mg/kg improved glucose toler-

ance in ICR mice, which exhibit normal insulin sensitivity. More importantly, in contrast to other TGR5 agonists reported to induce gallbladder filling as a major side effect[12], OL3 demonstrated no effect on gallbladder volume in ICR mice, even at the high dose of 300 mg/kg; a 50 mg/kg dose of MN6 significantly increased gallbladder volume. OL3 also reduced fasting blood glucose levels in *ob/ob* mice at doses of 200 and 400 mg/kg. A single oral dose of 400 mg/kg OL3 significantly improved glucose tolerance in *ob/ob* mice, but no obvious effect could be observed at the dose of 200 mg/kg. Because *ob/ob* mice exhibited severe insulin resistance[38, 39], higher doses of OL3 would be required to improve oral glucose tolerance compared to ICR mice. These data demonstrated that OL3 regulates glucose homeostasis in both normal and diabetic animal models. Our strategy to reduce systemic side effects by increasing the MW and tPSA of TGR5 agonists had been proved to be efficacious.

Given that OL3 was synthesized to incorporate linagliptin and exerted weak inhibition against DPP-4 *in vitro*, we investigated whether OL3 could inhibit DPP-4 *in vivo*. DPP-4 activity in serum was quantified during the OGTT in ICR mice, and a 26.17% DPP-4 inhibition rate was observed 1 h after an OL3 dose of 150 mg/kg. However, our results revealed that little OL3 was detected in the plasma, and the serum concentration of OL3 was too low to induce inhibition. Therefore, we speculated that linagliptin, which might be a metabolite of OL3, could contribute to DPP-4 inhibition *in vivo*. As demonstrated by pharmacokinetic data, the serum concentration of linagliptin was 0.19 ng/mL 1 h after oral administration of 150 mg/kg OL3. Because linagliptin is a potent DPP-4 inhibitor[24, 36] and the IC_{50} was as low as 2.91 nmol/L against mDPP-4 in our study, the linagliptin concentration in plasma could be sufficient to inhibit DPP-4. These results suggested that little OL3 absorbed into plasma was partially metabolized to linagliptin, which resulted in the *in vivo* inhibitory effects against DPP-4.

To further investigate the mechanism behind the glucose lowering effects of OL3, we evaluated the active form of GLP-1 in plasma in ICR mice. A comparable inhibition of DPP-4 by linagliptin to OL3 was set to exclude the increase in active GLP-1 induced by DPP-4 inhibition. OL3 not only exhibited a comparable inhibitory effect against DPP-4 but also led to an additional increase in the plasma active form of GLP-1 compared to linagliptin. These findings suggest that the increase in the active form of GLP-1 stimulated by OL3 was not only due to DPP-4 inhibition but was also the result of TGR5 activation. Together, these results revealed that OL3 improved glucose homeostasis in normal and diabetic animals, which was dependent on a synergistic increase in the active form of GLP-1 by activating TGR5 on intestinal L-cells and inhibiting DPP-4 activity in plasma.

In conclusion, by linking linagliptin to MN6, we generated the novel compound OL3, a low-absorbed compound with potent TGR5 activation and weak DPP-4 inhibition. OL3 demonstrated glucose lowering effects associated with an increase in the active form of GLP-1 in plasma. This increase was induced by TGR5 activation in the intestine and DPP-4 inhibition in plasma without gallbladder filling due to the low systemic exposure. Our study presents a new strategy in the development of TGR5 agonists targeted to the intestine to avoid systemic side effects in treating type 2 diabetes.

Acknowledgements

This work was financially supported by a grant from the National Natural Science Foundation of China (No 81473093), a grant from the State Key Laboratory of Drug Research (No SIMM1403ZZ-03) and a grant from the Shanghai Institute of Materia Medica (No CASIMM0120152030).

Author contribution

Ying LENG and Jian-hua SHEN designed the research; Shan-yao MA, Meng-meng NING, Qing-an ZOU, Ying FENG, and Yang-liang YE performed the research; Shan-yao MA, Meng-meng NING, Yang-liang YE, and Ying LENG wrote the paper.

References

1 Maruyama T, Miyamoto Y, Nakamura T, Tamai Y, Okada H, Sugiyama E, *et al.* Identification of membrane-type receptor for bile acids (M-BAR). Biochem Biophys Res Commun 2002; 298: 714–9.
2 Pols TW, Noriega LG, Nomura M, Auwerx J, Schoonjans K. The bile acid membrane receptor TGR5 as an emerging target in metabolism and inflammation. J Hepatol 2011; 54: 1263–72.
3 Kawamata Y, Fujii R, Hosoya M, Harada M, Yoshida H, Miwa M, *et al.* A G protein-coupled receptor responsive to bile acids. J Biol Chem 2003; 278: 9435–40.
4 Lieu T, Jayaweera G, Bunnett NW. GPBA: a GPCR for bile acids and an emerging therapeutic target for disorders of digestion and sensation. Br J Pharmacol 2014; 171: 1156–66.
5 Potthoff MJ, Potts A, He T, Duarte JA, Taussig R, Mangelsdorf DJ, *et al.* Colesevelam suppresses hepatic glycogenolysis by TGR5-mediated induction of GLP-1 action in DIO mice. Am J Physiol Gastrointest Liver Physiol 2013; 304: G371–80.
6 Katsuma S, Hirasawa A, Tsujimoto G. Bile acids promote glucagon-like peptide-1 secretion through TGR5 in a murine enteroendocrine cell line STC-1. Biochem Biophys Res Commun 2005; 329: 386–90.
7 Thomas C, Gioiello A, Noriega L, Strehle A, Oury J, Rizzo G, *et al.* TGR5-mediated bile acid sensing controls glucose homeostasis. Cell Metab 2009; 10: 167–77.
8 Parker HE, Wallis K, le Roux CW, Wong KY, Reimann F, Gribble FM. Molecular mechanisms underlying bile acid-stimulated glucagon-like peptide-1 secretion. Br J Pharmacol 2012; 165: 414–23.
9 Stoffers DA, Kieffer TJ, Hussain MA, Drucker DJ, Bonner-Weir S, Habener JF, *et al.* Insulinotropic glucagon-like peptide 1 agonists stimulate expression of homeodomain protein IDX-1 and increase islet size in mouse pancreas. Diabetes 2000; 49: 741–8.
10 Watanabe M, Houten SM, Mataki C, Christoffolete MA, Kim BW, Sato H, *et al.* Bile acids induce energy expenditure by promoting intracellular thyroid hormone activation. Nature 2006; 439: 484–9.
11 Watanabe M, Morimoto K, Houten SM, Kaneko-Iwasaki N, Sugizaki T, Horai Y, *et al.* Bile acid binding resin improves metabolic control through the induction of energy expenditure. PloS One 2012; 7: e38286.
12 Li T, Holmstrom SR, Kir S, Umetani M, Schmidt DR, Kliewer SA, *et al.* The G protein-coupled bile acid receptor, TGR5, stimulates gallbladder filling. Mol Endocrinol 2011; 25: 1066–71.

13 Lavoie B, Balemba OB, Godfrey C, Watson CA, Vassileva G, Corvera CU, *et al.* Hydrophobic bile salts inhibit gallbladder smooth muscle function via stimulation of GPBAR1 receptors and activation of K_{ATP} channels. J Physiol 2010; 588: 3295–305.
14 Stepanov V, Stankov K, Mikov M. The bile acid membrane receptor TGR5: a novel pharmacological target in metabolic, inflammatory and neoplastic disorders. J Receptor Signal Transduction Res 2013; 33: 213–23.
15 Fryer RM, Ng KJ, Nodop Mazurek SG, Patnaude L, Skow DJ, Muthukumarana A, *et al.* G protein-coupled bile acid receptor 1 stimulation mediates arterial vasodilation through a K(Ca)1.1 (BK(Ca))-dependent mechanism. J Pharmacol Exp Ther 2014; 348: 421–31.
16 Piotrowski DW, Futatsugi K, Warmus JS, Orr ST, Freeman-Cook KD, Londregan AT, *et al.* Identification of tetrahydropyrido[4,3-d]pyrimidine amides as a new class of orally bioavailable TGR5 agonists. ACS Med Chem Lett 2013; 4: 63–8.
17 Evans KA, Budzik BW, Ross SA, Wisnoski DD, Jin J, Rivero RA, *et al.* Discovery of 3-aryl-4-isoxazolecarboxamides as TGR5 receptor agonists. J Med Chem 2009; 52: 7962–5.
18 Harach T, Pols TW, Nomura M, Maida A, Watanabe M, Auwerx J, *et al.* TGR5 potentiates GLP-1 secretion in response to anionic exchange resins. Sci Rep 2012; 2: 430.
19 Duan H, Ning M, Chen X, Zou Q, Zhang L, Feng Y, *et al.* Design, synthesis, and antidiabetic activity of 4-phenoxynicotinamide and 4-phenoxypyrimidine-5-carboxamide derivatives as potent and orally efficacious TGR5 agonists. J Med Chem 2012; 55: 10475–89.
20 Duan H, Ning M, Zou Q, Ye Y, Feng Y, Zhang L, *et al.* Discovery of intestinal targeted TGR5 agonists for the treatment of type 2 diabetes. J Med Chem 2015; 58: 3315–28.
21 Lipinski CA, Lombardo F, Dominy BW, Feeney PJ. Experimental and computational approaches to estimate solubility and permeability in drug discovery and development settings. Adv Drug Delivery Rev 2001; 46: 3–26.
22 Pang Z, Nakagami H, Osako MK, Koriyama H, Nakagami F, Tomioka H, *et al.* Therapeutic vaccine against DPP4 improves glucose metabolism in mice. Proc Natl Acad Sci U S A 2014; 111: E1256–63.
23 Tella SH, Rendell MS. DPP–4 inhibitors: focus on safety. Expert Opin Drug Safety 2015; 14: 127–40.
24 Janardhan S, Sastry GN. Dipeptidyl peptidase IV inhibitors: a new paradigm in type 2 diabetes treatment. Curr Drug Targets 2014; 15: 600–21.
25 Brunton S. GLP-1 receptor agonists *vs* DPP-4 inhibitors for type 2 diabetes: is one approach more successful or preferable than the other? Int J Clin Practice 2014; 68: 557–67.
26 Thomas L, Eckhardt M, Langkopf E, Tadayyon M, Himmelsbach F, Mark M. (*R*)-8-(3-amino-piperidin-1-yl)-7-but-2-ynyl-3-methyl-1-(4-methyl-quinazolin-2-ylmethyl)-3,7-dihydro-purine-2,6-dione (BI 1356), a novel xanthine-based dipeptidyl peptidase 4 inhibitor, has a superior potency and longer duration of action compared with other dipeptidyl peptidase-4 inhibitors. J Pharmacol Exp Ther 2008; 325: 175–82.
27 Zou Q, Duan H, Ning M, Liu J, Feng Y, Zhang L, *et al.* 4-Benzofuranyloxynicotinamide derivatives are novel potent and orally available TGR5 agonists. Eur J Med Chem 2014; 82: 1–15.
28 Furuta Y, Horiguchi M, Sugaru E, Ono-Kishino M, Otani M, Sakai M, *et al.* Chronic administration of DSP-7238, a novel, potent, specific and substrate-selective DPP IV inhibitor, improves glycaemic control and beta-cell damage in diabetic mice. Diabetes Obesity Metab 2010; 12: 421–30.
29 Pellicciari R, Gioiello A, Macchiarulo A, Thomas C, Rosatelli E, Natalini B, *et al.* Discovery of 6alpha-ethyl-23(S)-methylcholic acid (S-EMCA, INT-777) as a potent and selective agonist for the TGR5 receptor, a novel target for diabesity. J Med Chem 2009; 52: 7958–61.
30 Deacon CF, Holst JJ. Linagliptin, a xanthine-based dipeptidyl peptidase-4 inhibitor with an unusual profile for the treatment of type 2 diabetes. Expert Opin Invest Drugs 2010; 19: 133–40.
31 Kim K, Park M, Lee YM, Rhyu MR, Kim HY. Ginsenoside metabolite compound K stimulates glucagon-like peptide-1 secretion in NCI-H716 cells via bile acid receptor activation. Arch Pharmacal Res 2014; 37: 1193–200.
32 Le Neve B, Daniel H. Selected tetrapeptides lead to a GLP-1 release from the human enteroendocrine cell line NCI-H716. Regul Peptides 2011; 167: 14–20.
33 Li YH, Bi HC, Huang L, Jin J, Zhong GP, Zhou XN, *et al.* Phorbol 12-myristate 13-acetate inhibits P-glycoprotein-mediated efflux of digoxin in MDCKII-MDR1 and Caco-2 cell monolayer models. Acta Pharmacol Sin 2014; 35: 283–91.
34 Duboc H, Tache Y, Hofmann AF. The bile acid TGR5 membrane receptor: from basic research to clinical application. Dig Liver Dis 2014; 46: 302–12.
35 Tiwari A, Maiti P. TGR5: an emerging bile acid G-protein-coupled receptor target for the potential treatment of metabolic disorders. Drug Discov Today 2009; 14: 523–30.
36 Barnett AH. Linagliptin for the treatment of type 2 diabetes mellitus: a drug safety evaluation. Expert Opin Drug Safety 2015; 14: 149–59.
37 Artursson P, Palm K, Luthman K. Caco-2 monolayers in experimental and theoretical predictions of drug transport. Adv Drug Delivery Rev 2001; 46: 27–43.
38 Haluzik M, Colombo C, Gavrilova O, Chua S, Wolf N, Chen M, *et al.* Genetic background (C57BL/6J versus FVB/N) strongly influences the severity of diabetes and insulin resistance in *ob/ob* mice. Endocrinology 2004; 145: 3258–64.
39 Liu X, Zhang LN, Feng Y, Zhang L, Qu H, Cao GQ, *et al*. Acute and chronic administration of SHR117887, a novel and specific dipeptidyl peptidase-4 inhibitor, improves metabolic control in diabetic rodent models. Acta Pharmacol Sin 2012; 33: 1013–2.